Mechanistic insight of SARS-CoV-2 infection using human hepatobiliary organoids

We have read with interest in a recent study published in Gut by Weber *et al*,[1] reporting abnormal elevation of gamma-glutamyltransferase (37%) and total bilirubin (5%) in patients, that was associated with higher rates of COVID-19-related deaths. However, whether SARS-CoV-2 could infect human hepatocytes and cholangiocytes thus causing local damage has not been reported. Here, human organoids were used to investigate SARS-CoV-2 infection and its induced liver damage at cellular and molecular levels (figure 1A).

We first established five lines of liver organoids and two lines of biliary organoids from adjacent normal tissues of seven patients with liver cancer (figure 1B; online supplemental figure 1A,B; online supplemental methods). We examined the susceptibility of human liver and biliary organoids to SARS-CoV-2 (Guangdong/20SF014/2020; EPI_ISL_403934; 19A) directly isolated from a patient with moderate COVID-19. The expression of SARS-CoV-2 spike (S) glycoprotein protein was readily detected in patchy areas of human liver and biliary organoids, but not in uninfected control by immunofluorescence staining (figure 1C; online supplemental figure 1C). Viral load of SARS-CoV-2 was dramatically increased in liver (liver 1 to liver 4) and biliary organoids (biliary 1 and biliary 2) at 24 hours postinfection with SARS-CoV-2, which remained stable for 96 hours in liver organoids and 48 hours in biliary organoids (figure 1D; online supplemental figure 2A; online supplemental table S1). Meanwhile, we found that live SARS-CoV-2 could amplify in lysed organoids (liver 5) and its culture supernatant (figure 1E; online supplemental table S1), inferring human liver and biliary organoids are susceptible to SARS-CoV-2 and support robust viral replication.

SARS-CoV-2 enters target cells mainly through the ACE2 receptor.[2] Given that ACE2 receptor was more highly expressed in cholangiocytes (59.7%) than in hepatocytes (2.6%),[3] we investigated the ultrastructure of SARS-CoV-2-infected biliary organoids under transmission electron microscopes (TEM) and found that viral particles were present in the lumen and at basolateral and apical sides of the organoid, as well as in membrane-bound vesicles (figure 2A). Therefore, TEM captured the critical location of SARS-CoV-2 in infected biliary organoids, indicating potential dissemination route of how SARS-CoV-2 enters the cholangiocytes.

Gene expression changes induced by SARS-CoV-2-infection in liver and biliary organoids was identified by RNA sequencing. Heatmap and volcano plot of differentially expressed genes revealed robust induction of proinflammatory chemokines/cytokines including CXCL1 in SARS-CoV-2-infected liver and biliary organoids. Consistently, KEGG Orthology Based Annotation System revealed multiple upregulated proinflammatory pathways in infected organoids, including NF-κB signalling pathway etc. Of note, the significant upregulation of TNF signalling pathway and apoptosis pathway in infection group indicated that SARS-CoV-2 infection may induce cell death of hepatocytes and cholangiocytes. Besides, UGT1A1 was upregulated in liver and biliary SARS-CoV-2-infected organoids, which was associated with elevation of bilirubin. While, bile acid transporter gene SLCO4C1 was significantly decreased in SARS-CoV-2-infected biliary organoid, and the steroid hormone biosynthesis and bile secretion pathways were upregulated in SARS-CoV-2-infected organoids, which could cause bile acid accumulation. Moreover, the upregulation of IL1R2 and IL1RL1 could be associated with the albumin production inhibition, thereby impairing liver functions.[4] It was reported an interacting host receptome of SARS-CoV-2 and demonstrated ASGR1 as alternative functional receptors, providing insight into SARS-CoV-2 tropism and pathogenesis.[5] We found that ASGR1 was upregulated in infected liver organoids, which may explain that SARS-CoV-2 viral load was higher in liver organoids compared with biliary organoids, though expression of ACE2 receptor was upregulated in cholangiocytes than hepatocytes (figure 2B–E; online supplemental figure 2B; online supplemental table S1). Consistently, bilirubin levels were reported to be significantly higher in non-survivors than survivors with SARS-CoV-2 infection.[1 6] Immunohistochemistry further validated the upregulated expressions of inflammatory factor CXCL8 and CXCL11 in SARS-CoV-2-infected biliary organoids

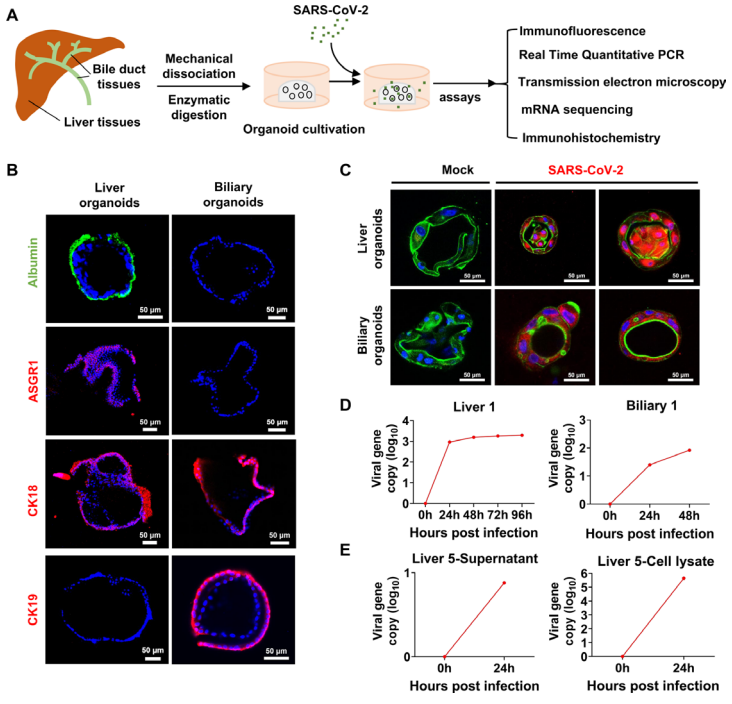

Figure 1 (A) Scheme of liver and biliary organoid culture establishment and performed assays. The liver and biliary organoids were generated from adjacent normal tissues of patients with liver cancer and coculture with SARS-CoV-2. (B) Differentiated liver and biliary organoids were immunostained using antibodies against human homologues to show albumin (green), ASGR1 (red), CK18 (red) and CK19 (red) protein, respectively. Nuclei are stained with DAPI (blue). Scale bar, 50 μm. (C) Immunofluorescent staining of SARS-CoV-2 infected liver organoids and biliary organoids at 24-hours. Virus are identified by SARS-CoV-2 spike (S) glycoprotein protein (red), nuclei and actin filaments are stained with DAPI (blue) and phalloidin (green), respectively. Scale bar, 50 μm. (D) Real time quantitative PCR analysis for viral sequences shows virus can productively replicate in the liver organoids at 0, 24, 48, 96 hours and in the biliary organoids at 0, 24, 48 hours after infection with SARS-CoV-2. (E) Live virus can be detected by RT-qPCR in supernatant and lysed organoids at 0 and 24 hours after infection with SARS-CoV-2.

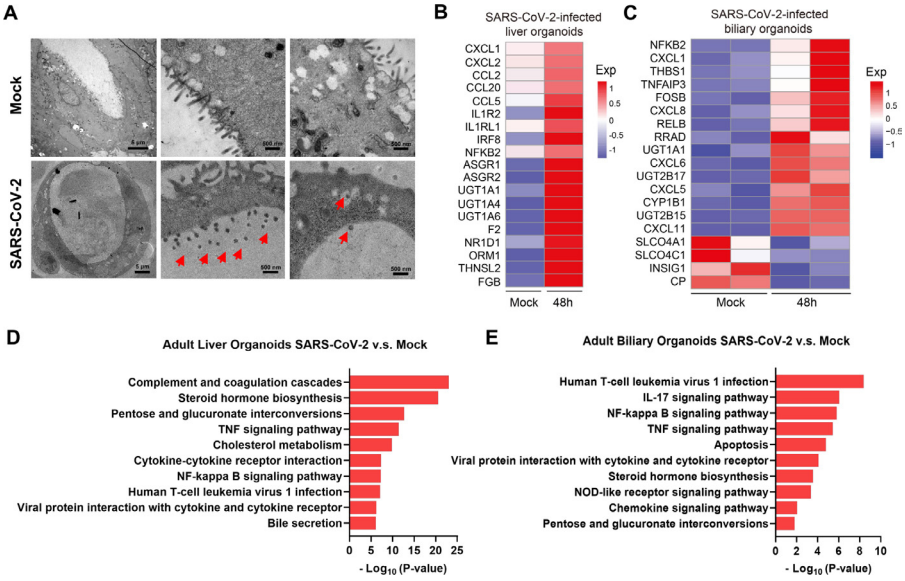

Figure 2 (A) Representative TEM imaging of biliary organoids at 0 and 24 hours of SARS-CoV-2 virus infection. Coronaviruses were observed in the lumen of the organoid (arrows) and are found at the membrane-bound vesicles (arrows). Scale bar 500 nm to 5 µm. (B, C) Heatmaps depicting the 19 most significantly enriched genes related to viral infection and immune system on SARS-CoV-2 infection in liver and biliary organoids. Coloured bar represents the log2-transformed values. (D, E) KEGG orthology-based annotation system of differential gene expression profiles from SARS-CoV-2-infected liver and biliary organoids compared with mock infection. TEM, transmission electron microscope.

compared with mock (online supplemental figure 2C).

In conclusion, SARS-CoV-2 can effectively infect human liver and biliary organoids. SARS-CoV-2 viruses are rapidly replicated in infected organoids to induce the production of proinflammatory cytokines/chemokines, local hepatocytes and cholangiocytes damage and consequent bile acid accumulation, which may contribute to liver injury.

Yi Zhao,[1,2] Xiaoxue Ren,[2,3] Jing Lu,[4] Minghui He,[1] Zhe Liu,[4] Lina Yi,[4] Mingle Huang,[1] Ming Kuang ,[1] Haipeng Xiao,[5] Joseph JY Sung ,[2,6] Xiaoxing Li ,[2] Lixia Xu,[2,3] Jun Yu [2,7]

[1]Department of Liver Surgery, Center of Hepato-Pancreato-Biliary Surgery, The First Affiliated Hospital, Sun Yat-sen University, Guangzhou, Guangdong, China
[2]Institute of Precision Medicine, The First Affiliated Hospital, Sun Yat-sen University, Guangzhou, Guangdong, China
[3]Department of Oncology, The First Affiliated Hospital, Sun Yat-sen University, Guangzhou, Guangdong, China
[4]Guangdong Provincial Institution of Public Health, Guangdong Provincial Center for Disease Control and Prevention, Guangzhou, Guangdong, China
[5]Department of Endocrinology, The First Affiliated Hospital,Sun Yat-sen University, Guangzhou, Guangdong, China
[6]Lee Kong Chian School of Medicine, Nanyang Technology University, Singapore
[7]Department of Medicine and Therapeutics and Institute of Digestive Disease, State Key Laboratory of Digestive Disease, The Chinese University of Hong Kong, Hong Kong SAR, China

Correspondence to Prof. Jun Yu, Department of Medicine and Therapeutics, State Key Laboratory of Digestive Disease, The Chinese University of Hong Kong, Shatin, N.T.,Hong Kong, China; junyu@cuhk.edu.hk, Prof. Lixia Xu, Department of Oncology, The First Affiliated Hospital,Sun Yat-sen University, Guangzhou, Guangdong, China; xulixia@mail.sysu.edu.cn and Prof. Xiaoxing Li, Institute of Precision Medicine, The First Affiliated Hospital, Sun Yat-sen University, Guangzhou, Guangdong, China; lixiaox23@mail.sysu.edu.cn

Contributors YZ and XR performed experiments and drafted the manuscript. JL performed experiments and revised the manuscript. MinghuiH and MingleH performed bioinformatics analyses. ZL and LY performed experiments. MK collected human samples and commented on the study. HX and JJYS supervised and commented on the study. XL, LX and JY designed, supervised the study and revised the manuscript.

Funding This work was supported by the National Natural Science Foundation of China (82173191), Guangdong Science and Technology Program (2021B1212030007).

Competing interests None declared.

Patient consent for publication Not applicable.

Ethics approval This study involves human participants and was approved by The Institutional Ethics Review Board of the First Affiliated Hospital, Sun Yat-Sen University. Participants gave informed consent to participate in the study before taking part.

Provenance and peer review Not commissioned; externally peer reviewed.

Supplemental material This content has been supplied by the author(s). It has not been vetted by BMJ Publishing Group Limited (BMJ) and may not have been peer-reviewed. Any opinions or recommendations discussed are solely those of the author(s) and are not endorsed by BMJ. BMJ disclaims all liability and responsibility arising from any reliance placed on the content. Where the content includes any translated material, BMJ does not warrant the accuracy and reliability of the translations (including but not limited to local regulations, clinical guidelines, terminology, drug names and drug dosages), and is not responsible for any error and/or omissions arising from translation and adaptation or otherwise.

► Additional supplemental material is published online only. To view, please visit the journal online (http://dx.doi.org/10.1136/gutjnl-2021-326617).

YZ, XR and JL contributed equally.

To cite Zhao Y, Ren X, Lu J, *et al*. *Gut* Epub ahead of print: [*please include* Day Month Year]. doi:10.1136/gutjnl-2021-326617

Received 21 November 2021
Accepted 7 April 2022

Gut 2022;**0**:1–2. doi:10.1136/gutjnl-2021-326617

ORCID iDs
Ming Kuang http://orcid.org/0000-0002-7397-5779
Joseph JY Sung http://orcid.org/0000-0003-3125-5199
Xiaoxing Li http://orcid.org/0000-0001-8791-7505
Jun Yu http://orcid.org/0000-0001-5008-2153

REFERENCES

1 Weber S, Hellmuth JC, Scherer C, *et al*. Liver function test abnormalities at hospital admission are associated with severe course of SARS-CoV-2 infection: a prospective cohort study. *Gut* 2021;70:1925–32.
2 Hoffmann M, Kleine-Weber H, Schroeder S, *et al*. SARS-CoV-2 cell entry depends on ACE2 and TMPRSS2 and is blocked by a clinically proven protease inhibitor. *Cell* 2020;181:271–80.
3 Chai X, Hu L, Zhang Y. Specific ACE2 expression in cholangiocytes may cause liver damage after 2019-nCoV infection. *bioRxiv* 2020.
4 Gounden V, Vashisht R, Jialal I. Hypoalbuminemia. In: *StatPearls*. Treasure Island (FL): StatPearls Publishing, 2022.
5 Gu Y, Cao J, Zhang X, *et al*. Receptome profiling identifies KREMEN1 and ASGR1 as alternative functional receptors of SARS-CoV-2. *Cell Res* 2022;32:24–37.
6 Jothimani D, Venugopal R, Abedin MF, *et al*. COVID-19 and the liver. *J Hepatol* 2020;73:1231–40.

Supplementary Figure 1

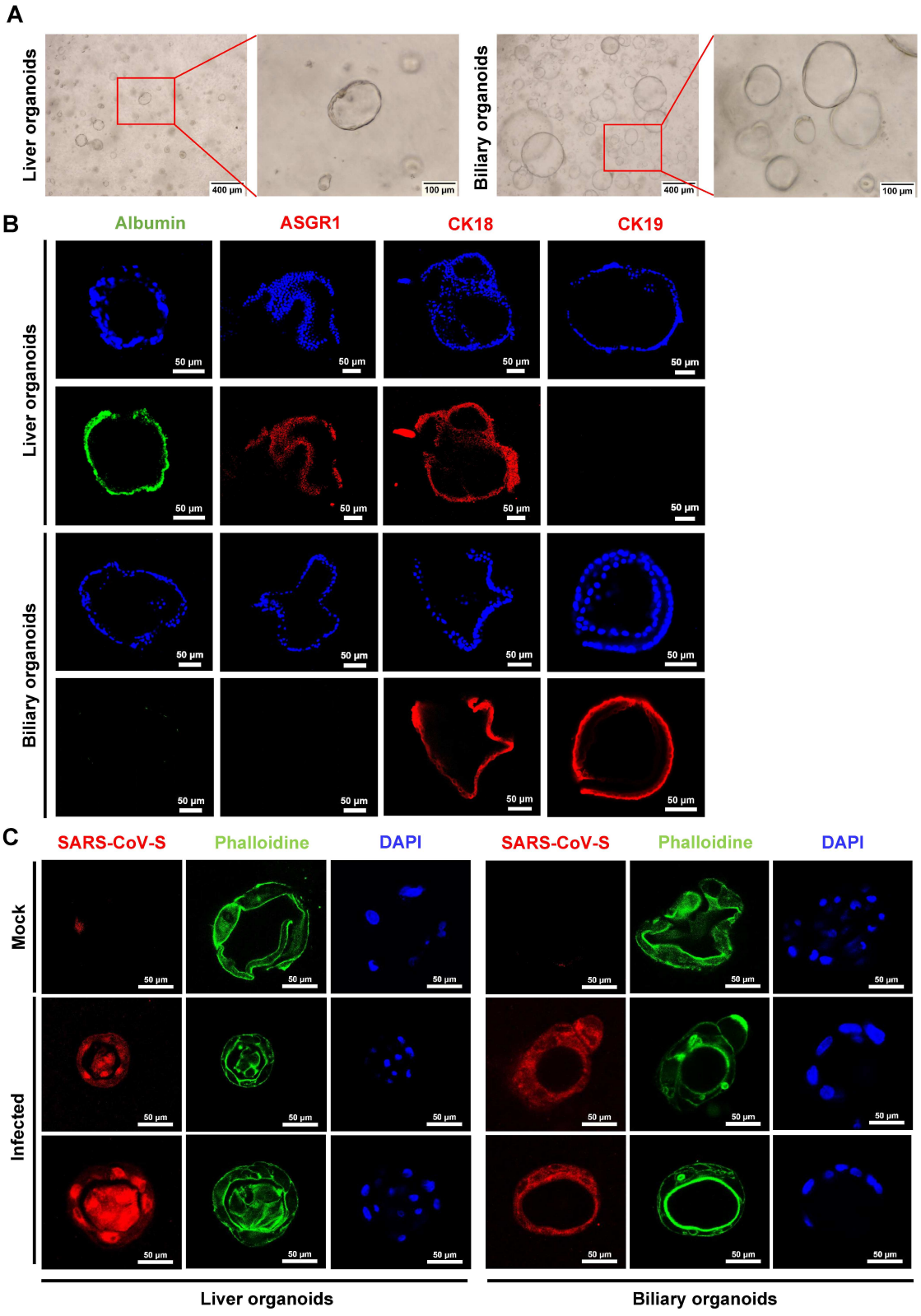

Supplementary Figure 1 (A) Representative bright field pictures of liver and biliary organoid. Note that, the liver and biliary organoids grew as a single-layered epithelium of ductal-like cells surrounding a central lumen. Scale bar, 100-400 μm. **(B)** Differentiated liver and biliary organoids were immunostained using antibodies against human homologues to show Albumin (green), ASGR1 (red), CK18 (red) and CK19 (red) protein, respectively. Nuclei are stained with DAPI (blue). Scale bar, 50 μm. **(C)** Immunofluorescent staining of SARS-CoV-2 infected liver organoids and biliary organoids. Virus are identified by SARS-CoV-2 spike (S) glycoprotein protein (red), Nuclei and actin filaments are stained with DAPI (blue) and Phalloidin (green), respectively. Scale bar, 50 μm.

Supplementary Figure 2

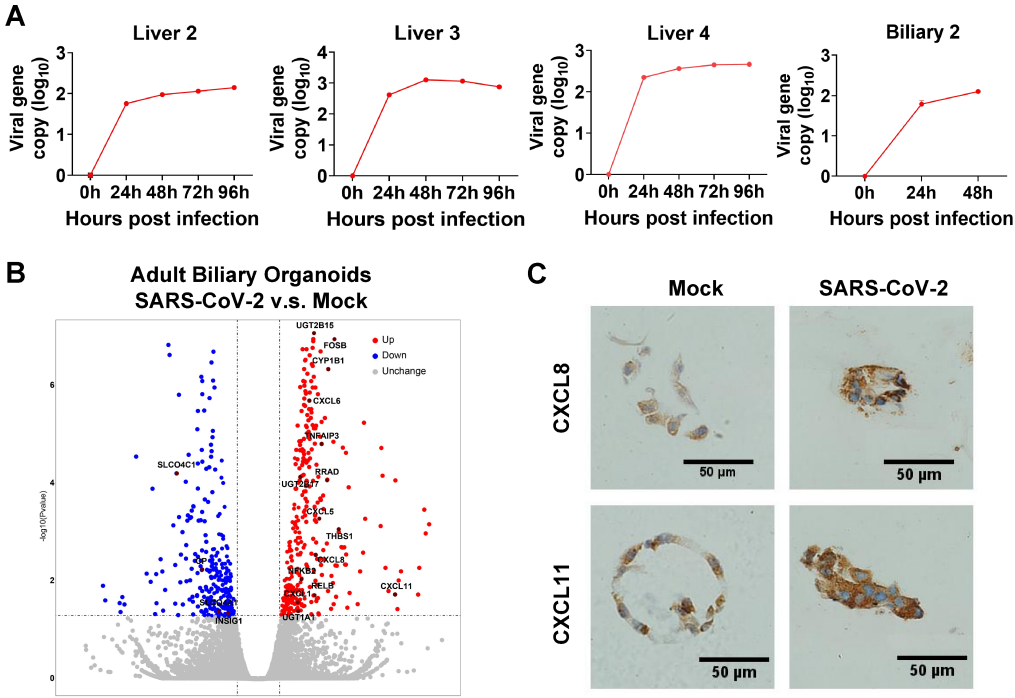

Supplementary Figure 2 **(A)** RT-qPCR analysis for viral sequences shows virus can productively replicate in the liver organoids at 0, 24, 48, 96 hours and in the biliary organoids at 0, 24, 48 hours after infection with SARS-CoV-2. **(B)** Volcano plot analysis of differentially expressed genes from SARS-CoV-2-infected biliary organoids compared to mock infection organoids. Individual genes denoted by gene name. Upregulated differentially expressed genes (p-adjusted value < 0.05) with a log2 (Fold Change) > 2 are indicated in red. Downregulated differentially expressed genes (p-adjusted value < 0.05) with a log2 (Fold Change) > 2 are indicated in blue. **(C)** Histopathologic staining of inflammatory markers (CXCL8 and CXCL11) of patient-derived biliary organoids at 0 hour and 24 hours of SARS-CoV-2 virus infection. Scale bar, 50 μm.

Supplementary methods

Patient samples

This study was approved by Ethics Committee of the First Affiliated Hospital of Sun Yat-Sen University. Liver and biliary organoids were derived from adjacent normal tissues in primary liver cancer patients who underwent surgical resection. Five lines of liver organoids and two lines of biliary organoids were collected from seven patients.

Cell culture of human liver and biliary organoids

Liver tissues of adult livers were dissected to ~1cm^3 sections and cut into pieces. Liver pieces were dissociated into single cells in Advanced DMEM/F12 (GIBCO) with collagenase, type IV (GIBCO) and dispase (Corning) for 1 hour in 37°C with gentle shaking. After filtering, hepatocytes were resuspended in 200 μL of growth factor reduced Matrigel (Corning) and plated in ~30 μL droplets in a 48-well tissue culture plate. The expansion medium was used for 5 days, then replaced by the medium with fresh differentiation medium for 15 days to differentiate organoids into hepatocytes. The expansion medium contained Advanced DMEM/F12 supplemented with 1% penicillin/streptomycin, 1% Glutamax, 10 mM HEPES, 1:50 B27 supplement (without vitamin A), 1:100 N2 supplement, 1.25 mM N-acetyl-L-cysteine, 10% (vol/vol) Rspo-1 conditioned medium, 10% (vol/vol) WNT3a-conditioned medium, 10 mM nicotinamide, 10 nM gastrin I, 50 ng/ml recombinant human EGF, 100 ng/ml recombinant human FGF10, 25 ng/ml recombinant human HGF, 10 μM forskolin, 5 μM A8301, 25 ng/ml Noggin and 10 μM Y27632. The human liver differentiation medium is the expansion medium supplemented with 10 μM DAPT, 3 μM dexamethasone, 25 ng/ml BMP7 and 100 ng/ml recombinant human FGF19, as described previously [1]. The medium was changed every 5 days.

Biliary tract tissues were received intact and the wall of the ducts was incised with a scalpel to expose the lumen. The mucosal surface was then abraded with a scalpel to

mechanically dissociate the epithelium. For organoid derivation, epithelium was resuspended in GFR Matrigel. Droplets (30 μL) were plated per well into a 48-well plate. The medium contained Advanced DMEM/F12 supplemented with 1% penicillin/streptomycin, 1% Glutamax, 10 mM HEPES, 1:50 B27 supplement (without vitamin A), 1:100 N2 supplement, 1.25 mM N-acetyl-L-cysteine, 10% (vol/vol) Rspo-1 conditioned medium, 10 mM nicotinamide, 10 nM gastrin I, 50 ng/ml recombinant human EGF, 10 μM forskolin, 5 μM A8301 and 10 μM Y27632, as described previously [2].

For passaging, organoids were dissociated into single cells using TrypLE express (GIBCO). After 3 passages, cultures were used for infection experiments.

Virus stock preparation

SARS-CoV-2 (isolate Guangdong/20SF014/2020; EPI_ISL_403934) was propagated on Vero E6 cells in MEM (Gibco), supplemented with 2% FBS, penicillin (10,000 IU/mL) and streptomycin (10,000 IU/mL). The culture supernatant was collected when CPE (cytopathic effect) was observed on ~80% cells. The supernatant was cleared by centrifugation and stored in aliquots at −80°C. Stock titers were determined according to the method of Spearman & Kärber. SARS-CoV-2 virus propagation and infection was performed in the BSL-3 laboratory of Guangdong Provincial Center for Diseases Control and Prevention.

SARS-CoV-2 infection

Organoids were infected at MOI of 1 in organoid culture medium. Time was set as zero when organoids were initially incubated with viruses. After 1 hour adsorption, culture media were removed and organoids were washed twice with ice cold PBS to remove unattached virus, then re-embedded in Matrigel and maintained in the culture medium. Supernatant and organoid samples were collected at different timepoints after inoculation.

Determination of virus titers using RT-qPCR

Viral RNA in supernatant and organoid samples was extracted by using Viral RNA minikit (Qiagen, Germany). Relative viral loads were calculated by using SARS-CoV-2 quantitative reverse-transcription PCR (RT-qPCR) kit (Daan Gene, Guangzhou, China). RT-qPCR assays were set up in triplicate. All protocols were performed according to the manufactures' instructions. Results were analyzed with the ΔΔCT method.

Immunofluorescence and immunohistochemistry

For whole mounting liver and biliary organoids staining, organoids were fixed in 4% paraformaldehyde and permeabilized with 0.3% Triton X-100 (biosharp, X100) in PBS, then blocked by 10% goat serum in PBS. Organoids were then incubated with mouse anti-SARS-CoV-2 S protein (prepared by Guangdong Provincial Center for Diseases Control and Prevention, 1:200), Albumin (Proteintech, 66051-1-Ig, 1:50), CK18 (Invitrogen, PA5-14263, 1:25), ASGR1 (Abcam, ab254261, 1:50), CK19 (Abcam, ab76539, 1:1000) at 4 °C overnight, and then incubated with mouse IgG (H+L) cross-adsorbed secondary antibody (Invitrogen, A11003, 1:500) and rabbit IgG (H+L) cross-adsorbed secondary antibody (Invitrogen, A32723, 1:1000), and phalloidin (Sigma, P5282, 1:300) at room temperature. Organoids were eventually incubated with DAPI. Imaging was performed on Multiphoton Microscope STELLARIS 8 DIVE (Leica, Germany).

Immunohistochemistry was performed on 4 μm sections of paraffin-embedded organoids. Immunostaining for CXCL8 (Proteintech, Cat No. 27095-1-AP,1:500) and CXCL11(Abcam, ab9955, 1:1000) proteins were performed for patient-derived biliary organoids at 0 hour and 24 hours after SARS-CoV-2 infection. Images were acquired on OLYMPUS BX63F microscope.

Transmission electron microscopy

Organoids were fixed with 2.5% glutaraldehyde in 0.1M PBS to pH 7.4 and 2% paraformaldehyde at 4 °C overnight. Organoids were then dehydrated at room temperature in a graded ethanol series (30, 50, 70, 80, 90, and 100%) and embedded in epon812. Epon was polymerized for 48h at 60°C. Ultrathin sections at 70nm were cut using a diamond knife (Diatome) on a Leica UC7 ultramicrotome, and transferred onto 200 Mesh copper grids covered with a formvar and carbon film. Sections were post-stained with uranyl acetate and lead citrate. All TEM data were collected by transmission electron microscope (FEI Tecanai G2 Spirit Twin, USA)

Bulk RNA sequencing

Total RNA was extracted from biliary organoids by RNeasy Mini Kit (Qiagen, Germany). Beads (Invitrogen) with oligo (dT) were used to isolate poly (A) mRNA after total RNA was collected. Fragmentation buffer was added for interrupting mRNA to obtain short fragments. Using these short fragments as templates, random hexamer-primer was used to synthesize the first-strand cDNA. The second-strand cDNA was synthesized using buffer, dNTPs, RNase H, and DNA polymerase I. Short fragments were purified with QIAQuick PCR Extraction Kit (Qiagen) and resolved in EB buffer for end reparation and adding poly (A). After that, the short fragments were connected to sequencing adaptors. For PCR amplification, suitable fragments were selected as templates based on agarose gel electrophoresis. The library was sequenced using HiSeq X TEN platform and 150-bp paired-end reads were generated.

mRNA sequencing data analysis

Gene differential expression analysis between normal controls and 48h group was performed by the R DESeq package using count data of high-throughput sequencing. DESeq result was filtered by p value (< 0.05) and fold change (> 2). Ensembl ID of differentially expressed genes was then converted to Entrez ID by the R org.Hs.eg.db package and submitted to the R clusterProfiler package to perform KEGG pathway enrichment. From the KEGG pathway enrichment result, significant KEGG pathways (p value < 0.05) related to viral infection and immune system were selected for further

investigation. The heatmap plot of gene expressions, the volcano plot of result of gene differential expression analysis, and the bar plot of pathways were generated using the R ggplot2 package.

Statistical analysis

Error bars in these figures indicate S.D. (for RT-qPCR). Student's t-test or ANOVA test was employed to compare between two groups of n = 3 or more samples. $P < 0.05$ was defined as statistical significance. All of the statistical analyses in this study were done with GraphPad Prism 8 software.

References

[1] Broutier L, Andersson-Rolf A, Hindley CJ, et al. Culture and establishment of self-renewing human and mouse adult liver and pancreas 3D organoids and their genetic manipulation. Nat Protoc. 2016;11:1724-43.

[2] Tysoe OC, Justin AW, Brevini T, et al. Isolation and propagation of primary human cholangiocyte organoids for the generation of bioengineered biliary tissue. Nat Protoc. 2019;14:1884-1925.